
Article:
Abdulmajid, A.A., Khamas, S. and Zhang, S. (2020) Wide bandwidth high gain circularly polarized millimetre-wave rectangular dielectric resonator antenna. Progress In Electromagnetics Research M, 89. pp. 171-177. ISSN 1937-8726

https://doi.org/10.2528/pierm19111903

Progress In Electromagnetics Research M, Vol. 89, 171–177, 2020

Wide Bandwidth High Gain Circularly Polarized Millimetre-Wave Rectangular Dielectric Resonator Antenna

Abdulmajid A. Abdulmajid[1, *], Salam Khamas[1], and Shiyu Zhang[2]

Abstract—A wideband high gain circularly polarized (CP) rectangular dielectric resonator antenna (RDRA) having a frequency range of 21 to 31 GHz is proposed. The RDRA consists of two layers with different dielectric permittivities and has been excited using a cross slot aperture. The proposed antenna offers wide impedance and CP bandwidths of ∼36.5 % and 13.75%, respectively, in conjunction with a high gain of ∼12.5 dBi. Close agreement has been achieved between simulated and measured results.

1. INTRODUCTION

Wireless communication systems have grown dramatically over the last few decades. As a result, the carrier frequencies have been shifted up to the mm-wave band in order to acquire a much wider bandwidth and minimize the interference in the overcrowded lower frequencies' spectrum. With the increasing demands for wireless mobile devices and services, the new wireless applications require high data rates in the order of 1 Gbps that can only be supported by the fourth generation (4G) wireless networks [1]. Therefore, the mm-wave frequency band has been utilized in the fifth generation (5G) wireless systems in order to achieve higher data rates [1, 2]. Further, mm-waves signals have the ability of penetration through fog and heavy dust [3]. However, the electromagnetic energy at the mm-wave band can be absorbed by oxygen, which attenuates the signal over the communications channel and necessitates the use of a high gain antenna [4]. Unfortunately, antenna arrays require feed networks with potentially high ohmic losses at higher frequencies as well as increased cost, size and complexity. Furthermore, microstrip antennas are associated with well-known limitations such as narrow impedance bandwidths and considerably lower gain due to ohmic and surface wave losses at the mm-wave frequency range [5]. Therefore, a DRA represents a suitable choice to address the aforementioned limitations as it offers wide bandwidth in conjunction with high radiation efficiency of more than 90%, as well as other appealing features such as small size, various geometries, easy excitation, low profile and lightweight [6, 7]. As a result, millimetre wave DRAs have been the focus of several recent studies [8–12]. In addition, a number of studies have focused on the design of mm-wave DRA arrays [13–16]. As the higher order mode DRAs increase the effective permittivity then a narrower impedance bandwidth is expected [3]. The outer layer creates a transition region between the antenna and air resulting in an enhanced impedance bandwidth. In addition, the dielectric coat serves another purpose by exciting additional resonance modes in the same band, and margining the bands of adjacent modes improves the impedance bandwidth further. It is worth pointing that wideband and high gain X-band DRAs have been reported recently by incorporating an outer dielectric coat layer [17, 18]. This approach is utilized in this letter for the mm-wave band applications, where further performance improvements have been achieved by optimizing the feed network and the dielectric coat dimensions. The simulations have been implemented using the time domain solver of CST microwave studio [19].

Received 19 November 2019, Accepted 17 January 2020, Scheduled 3 February 2020

* Corresponding author: Abdulmajid A. Abdulmajid (aaaabdulmajid1@sheffield.ac.uk).

[1] Department of Electrical Engineering and Electronics, University of Sheffield, Sheffield, S1 4DT, UK. [2] School of Mechanical, Electrical and Manufacturing Engineering, Loughborough, LE11 3TU, UK.

2. THEORY

For a single layer DRA, the resonance frequency of each TE_{mnp} mode can be calculated using the dielectric wave guide model, DWM [20], which results in the following equations

$$kx = \frac{m\pi}{w}$$
$$ky = \frac{n\pi}{l}$$
$$kz \tan\left(\frac{kzh}{2}\right) = \sqrt{((\epsilon r - 1)k0^2 - kx^2)}$$
$$kx^2 + ky^2 + kz^2 = \epsilon r k0^2 \quad (1)$$
$$k0 = \frac{2\pi}{\lambda 0} = \frac{2\pi f0}{c} \quad (2)$$

in which $\lambda 0$ is the free-space wavelength, and c is the speed of light. Substitution of Equation (2) in Equation (1) provides an equation to calculate the modes' resonance frequency as:

$$f0 = \frac{c}{2\pi\epsilon r}\sqrt{(kx^2 + ky^2 + kz^2)} \quad (3)$$

However, there is no equivalent equation for a layered DRA structure. Hence the CST Eigen mode solver has been utilized to predict the resonance frequencies of various modes in layered DRA configuration.

3. ANTENNA CONFIGURATION

In this work, a mm-wave rectangular DRA working at higher order modes is designed and measured. Fig. 1 illustrates the proposed RDRA geometry with an inner layer dimensions of l_1=w_1=2 mm and h_1=10 mm as well as a relative permittivity of ϵ_{r1}= 10. The DRA has been coated by a Polyamide outer layer that has dimensions of l_2=w_2=12 mm and h_2 =11 mm with a dielectric constant of ϵ_{r2}= 10= 3.5. The proposed antenna has been placed on a Rogers RO4535 substrate having size of 200 mm^2, thickness of 0.5 mm and dielectric constant of 3.5. In addition, a cross-slot with unequal arm lengths of ls_1=1.9 and ls_2=2.6 mm and identical width of ws_1=ws_2=0.5 mm has been etched on the ground plane in order to generate two near resonant modes having an equal amplitude and 90°. phase difference that are required to generate the circular polarization [21, 22]. The reflection coefficient has been measured

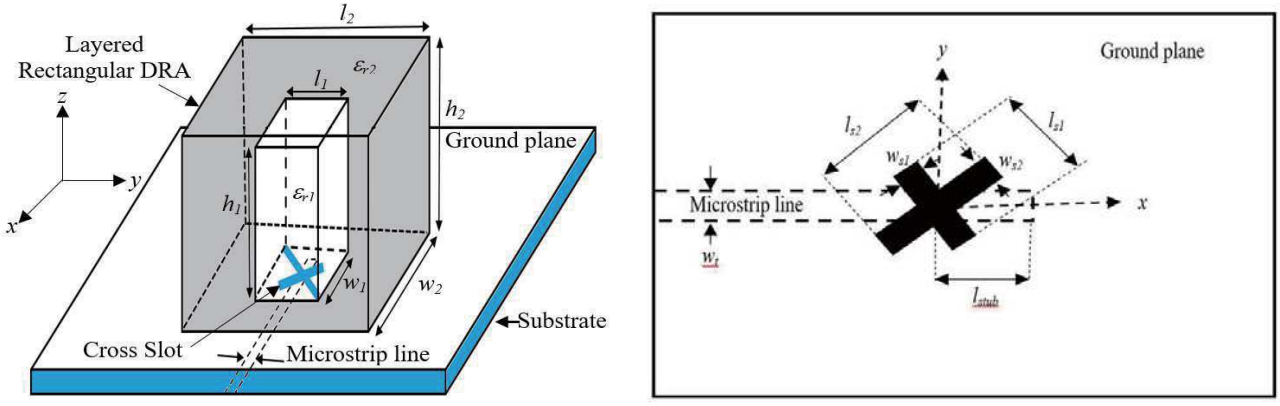

Figure 1. Configuration of mm-wave layered rectangular DRA excited by cross slot, (a) layered RDRA, (b) cross slot feeding.

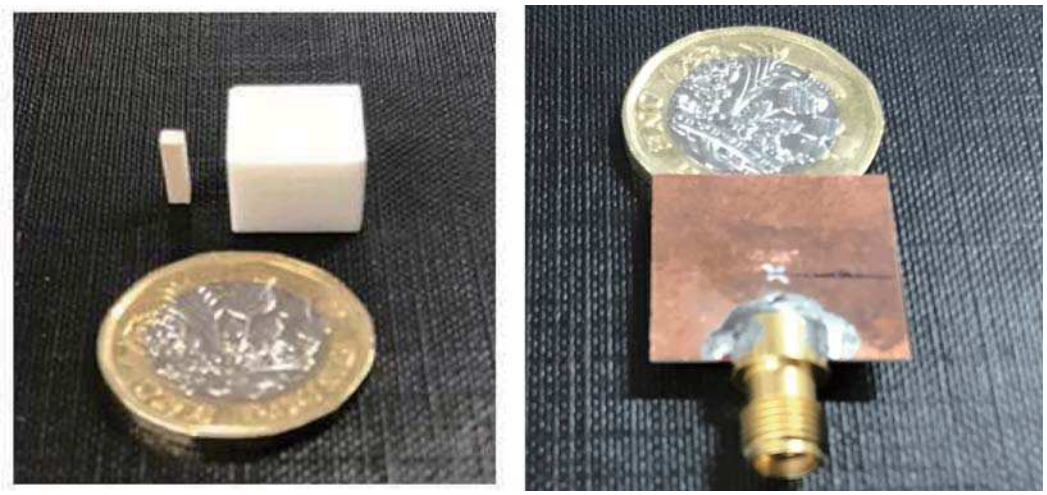

(a) (b)

Figure 2. Layered mm-wave rectangular DRA excited by cross slot; (a) DRA and coat, (b) feed network.

using an E5071C vector network analyzer thorough a 50 Ω coaxial cable. A 2.92 mm SMA has been utilized between the coaxial cable and the feeding strip line. The calibration has been carried out using the Agilent's 85052D calibration kit. The radiation patterns have been measured using the SNF-FIX-1.0 Spherical Near-field mm-Wave Measurement System. The prototype of the DRAs is shown in Fig. 2.

4. RESULTS AND DISCUSSION

Figure 3 demonstrates a close agreement between the simulated and measured return losses with respective bandwidths of 36.5% and 35.6% over a simulated frequency range of 21.5 to 31.1 GHz that agrees well with a measured range of 21.7 to 31.1 GHz. From these results, it can be noted the DRA supports a multi-higher order modes operation since the following resonance modes have been excited; TE_{115}, TE_{117} and TE_{119} at 22.5 GHz, 27 GHz and 29.5 GHz, respectively. Fig. 4 illustrates the normalized E-plane and H-plane far field patterns with close agreement between simulated and measured

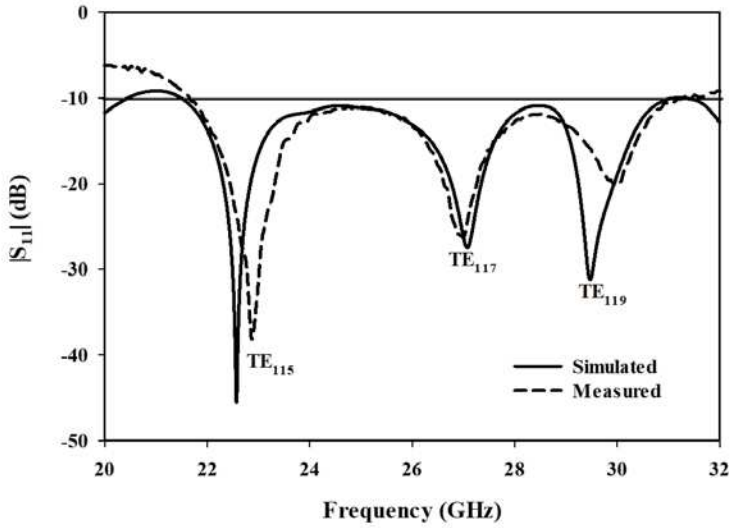

Figure 3. Simulated and measured return loss of a layered mm-wave RDRA.

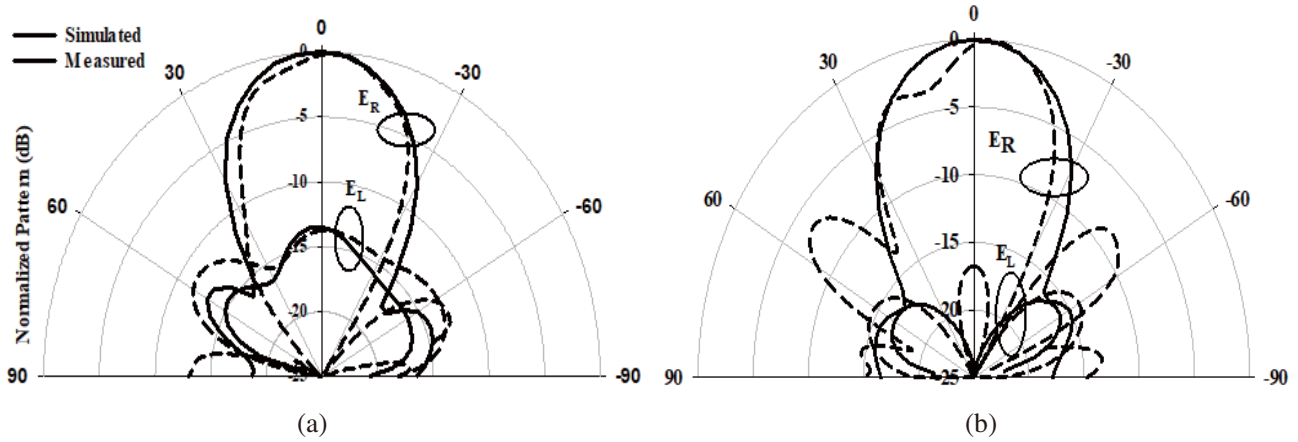

Figure 4. Simulated and measured normalized radiation patterns for TE_{115} at 24 GHz (a) E-plane, (b) H-plane.

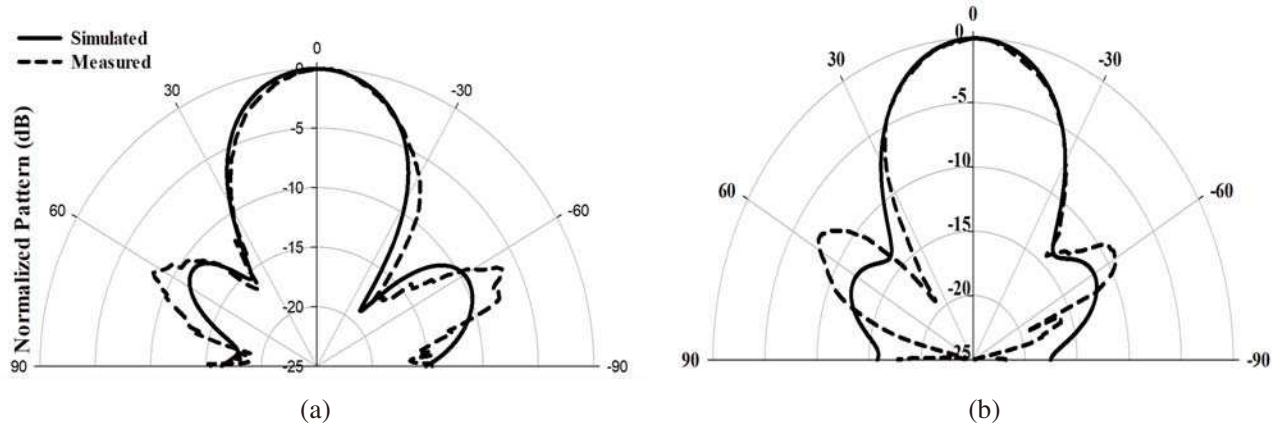

Figure 5. Simulated and measured normalized radiation patterns for TE_{117} at 27 GHz (a) E-plane, (b) H-plane.

results with measured and simulated gains 12.5 and 12.1 dBic, respectively, which demonstrate a right hand circularly polarized (RHCP) antenna since E_R is considerably higher than E_L. However, the minor disagreements between the simulated and measured H-plane patterns could be attributed to fabrication and measurements tolerances. It is worth mentioning that a right-hand circular polarization sense, RHCP, has been achieved due to the fact that the length of the ls_2 arm of the cross slot is longer than ls_1 as demonstrated in Fig. 1(b). Similarly, left hand circular polarization, LHCP, can be achieved by swapping the cross-slot arms so that ls_1 is longer. The simulated and measured radiation patterns of TE_{115}, TE_{117} and TE_{119} modes are illustrated in Figs. 4, 5, and 6 at 24, 27.5 and 29 GHz, respectively. These results demonstrate the stability and consistent of the radiation patterns, which is expected since all the excited modes offer broad side far field patterns. The simulated and measured axial ratios and directivities agree well with each other as demonstrated in Fig. 7. It can be noted that both of the measured and simulated CP radiations have been acquired over a frequency range of 23.4-26.7 GHz, which corresponds to an AR bandwidth of 13.7% . This has been achieved in conjunction with a stable directivity across the circular polarization bandwidth with a maximum of ∼12.5 dBi at 24 GHz in both of the simulated and measured data. It is worth pointing that, the wider axial ratio band has been acquired due to the combination of TE_{115} and TE_{117} modes. It should be noted that at the absence of the Polyimide coating layer, the DRA directivity, impedance, and AR bandwidths are 8.66 dBi, 7.5%, and 1.95%, respectively. Furthermore, Table 1 presents a comparison between the performances of the

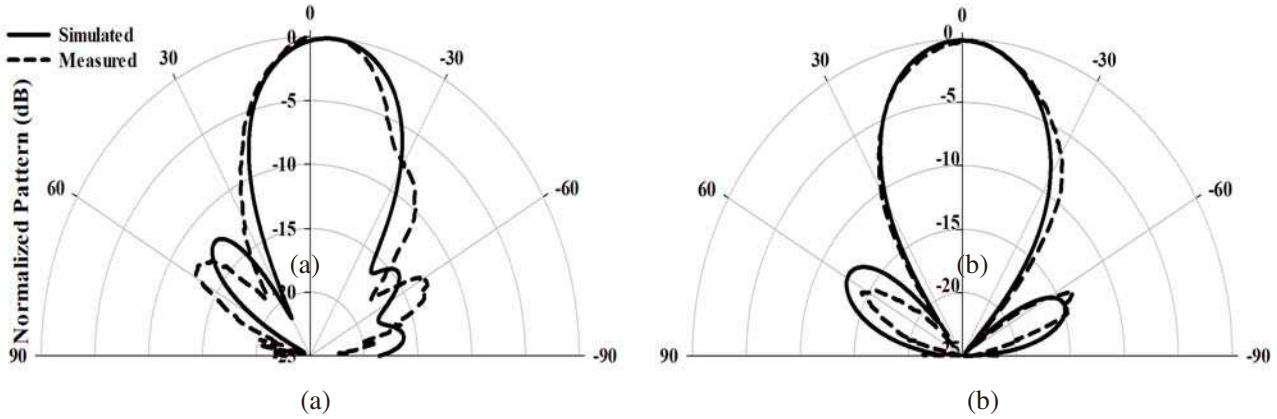

Figure 6. Simulated and measured normalized radiation patterns for TE_{119} at 29.5 GHz (a) E-plane, (b) H-plane.

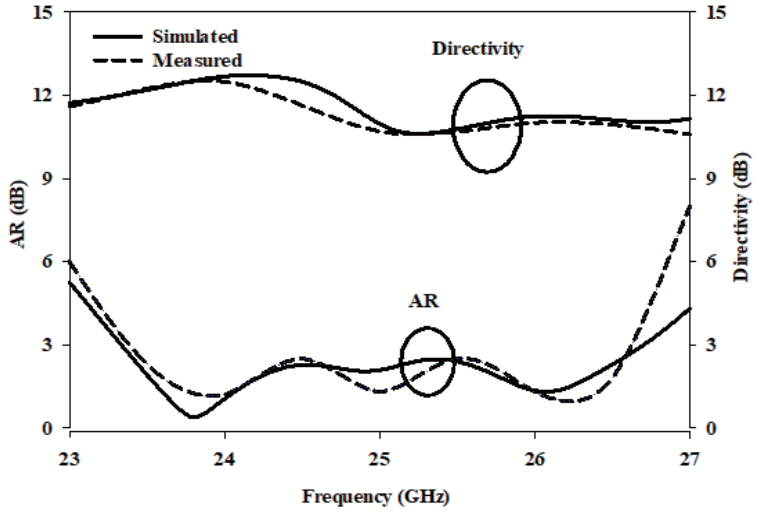

Figure 7. Simulated and measured axial ratios and directivities for layered mm-wave RDRA.

Table 1. Comparison between the performances of the proposed antenna with a number of DRA arrays.

References	Number of elements	Frequency (GHz)	Gain (dBi)	S_{11} Bandwidth (%)	Axial Ratio Bandwidth (%)
Proposed antenna	1	21.5–31	12.5	36.3	13.7
[14]	6 × 8	59–61	18	3.33	1.64
[15]	4	27–31	18	26.8	11.9
[16]	4	28–36	12	10	-

proposed layered DRA to that of a several DRA arrays [13–16]. From the tabulated data, it can be noted that the performance of the presented antenna is comparable to those of the arrays albeit with the utilization of a single element, which results in a smaller overall size as well as the absence of an array feed network.

5. CONCLUSION

A two-layer mm-wave DRA configuration has been investigated and measured. The proposed antenna offers a high gain of ∼12.5 dBi in conjunction with wider impedance and axial ratio bandwidths of 36.5% and 13.7%, respectively. The improved bandwidth has been achieved due to the excitation of multiple higher order modes as a result of incorporating a dielectric coat layer. On the other hand, the gain has been enhanced due to the increased order of the excited DRA modes at the presence of the coat layer. In addition to the performance improvements, the outer dielectric layer has provided a physical support due to the small DRA size as well as an easy holder to the DRA on the ground plane. Furthermore, the radiation characteristics of the layered DRA are comparable to those of a number of DRA arrays that have been reported in the literature. The appealing features of the presented antenna can play a major role for 5G applications that require directive antennas with wider bandwidth.

REFERENCES

1. Niu, Y., Y. Li, D. Jin, L. Su, and A. V. Vasilakos, "A survey of millimeter wave communications (mmWave) for 5G: Opportunities and challenges," *Wireless Networks*, Vol. 21, 2657–2676, 2015.
2. Wang, C.-X., F. Haider, X. Gao, X.-H. You, Y. Yang, D. Yuan, et al., "Cellular architecture and key technologies for 5G wireless communication networks," *IEEE Communications Magazine*, Vol. 52, 122–130, 2014.
3. Pan, Y.-M., K. W. Leung, and K.-M. Luk, "Design of the millimeter-wave rectangular dielectric resonator antenna using a higher-order mode," *IEEE Transactions on Antennas and Propagation*, Vol. 59, 2780–2788, 2011.
4. Shahadan, N. H., M. H. Jamaluddin, M. R. Kamarudin, Y. Yamada, M. Khalily, M. Jusoh, et al., "Steerable higher order mode dielectric resonator antenna with parasitic elements for 5G applications," *IEEE Access*, Vol. 5, 22234–22243, 2017.
5. Luk, K. M. and K. W. Leung, *Dielectric Resonator Antennas*, Research Studies Press Limited, Hertforodshire, England, UK, 2002.
6. Gangwar, R. K., S. Singh, and D. Kumar, "Comparative studies of rectangular dielectric resonator antenna with probe and microstrip line feeds," *Archives of Applied Science Research*, Vol. 2, 1–10, 2010.
7. Petosa, A. and S. Thirakoune, "Rectangular dielectric resonator antennas with enhanced gain," *IEEE Transactions on Antennas and Propagation*, Vol. 59, 1385–1389, 2011.
8. Oh, J., T. Baek, D. Shin, J. Rhee, and S. Nam, "60-GHz CPW-fed dielectric-resonator-above-patch (DRAP) antenna for broadband WLAN applications using micromachining technology," *Microwave and Optical Technology Letters*, Vol. 49, 1859–1861, 2007.
9. Elboushi, A., O. Haraz, A. Sebak, and T. Denidni, "A new circularly polarized high gain DRA millimeter-wave antenna," *2010 IEEE in Antennas and Propagation Society International Symposium (APSURSI)*, 1–4, 2010.
10. Perron, A., T. A. Denidni, and A. R. Sebak, "Circularly polarized microstrip/elliptical dielectric ring resonator antenna for millimeter-wave applications," *IEEE Antennas and Wireless Propagation Letters*, Vol. 9, 783–786, 2010.
11. Feng, L. Y. and K. W. Leung, "Millimeter-wave wideband dielectric resonator antenna," *2015 40th International Conference on Infrared, Millimeter, and Terahertz waves (IRMMW-THz)*, 1–2, 2015.
12. Laribi, M. and N. Hakem, "Hight-gain circular polarised hybrid DRA for millimeter-wave," *IEEE International Symposium on Antennas and Propagation (APSURSI)*, 141–142, 2016.
13. Nor, N. M., M. H. Jamaluddin, M. R. Kamarudin, and M. Khalily, "Rectangular dielectric resonator antenna array for 28 GHz applications," *Progress In Electromagnetics Research C*, Vol. 63, 53–61, 2016.
14. Kaouach, H., L. Dussopt, J. Lanteri, T. Koleck, and R. Sauleau, "Wideband low-loss linear and circular polarization transmit-arrays in V-band," *IEEE Transactions on Antennas and Propagation*, Vol. 59, 2513–2523, 2011.

15. Lin, J.-H., W.-H. Shen, Z.-D. Shi, and S.-S. Zhong, "Circularly polarized dielectric resonator antenna arrays with fractal cross-slot-coupled DRA elements," *International Journal of Antennas and Propagation*, Vol. 2017, 2017.
16. Mazhar, W., D. Klymyshyn, G. Wells, A. Qureshi, M. Jacobs, and S. Achenbach, "Low profile artificial grid dielectric resonator antenna arrays for mm-wave applications," *IEEE Transactions on Antennas and Propagation*, Vol. 67, 4406–4417, 2019.
17. Abdulmajid, A. A., Y. Khalil, and S. Khamas, "Higher-order-mode circularly polarized two-layer rectangular dielectric resonator antenna," *IEEE Antennas and Wireless Propagation Letters*, Vol. 17, 1114–1117, 2018.
18. Abdulmajid, A. A. and S. Khamas, "Higher order mode layered cylindrical dielectric resonator antenna," *Progress In Electromagnetics Research C*, Vol. 90, 65–77, 2019.
19. Studio, M., "Computer simulation technology (CST)," Online: www.cst.com, 2015.
20. Maity, S. and B. Gupta, "Closed form expressions to find radiation patterns of rectangular dielectric resonator antennas for various modes," *IEEE Transactions on Antennas and Propagation*, Vol. 62, 6524–6527, 2014.
21. Almpanis, G., C. Fumeaux, and R. Vahldieck, "Offset cross-slot-coupled dielectric resonator antenna for circular polarization," *IEEE Microwave and Wireless Components Letters*, Vol. 16, 461–463, 2006.
22. Maknikar, R. D. and V. G. Kasabegoudar, "Circularly polarized cross-slot-coupled stacked dielectric resonator antenna for wireless applications," *International Journal of Wireless Communications and Mobile Computing*, Vol. 1, 68–73, 2013.